Published in final edited form as:
Neurosci Lett. 2009 January 30; 450(2): 191–195. doi:10.1016/j.neulet.2008.11.017.

Axon sprouting in adult mouse spinal cord after motor cortex stroke

Christine M. LaPash Daniels[1], **Kathryn L. Ayers**[1], **Amanda M. Finley**[1], **Joseph P. Culver**[2], and **Mark P. Goldberg**[1]

[1]Department of Neurology and Hope Center for Neurological Disorders Washington University School of Medicine, 660 S. Euclid Ave., St. Louis, Missouri 63110.

[2]Department of Radiology Washington University School of Medicine, 660 S. Euclid Ave., St. Louis, Missouri 63110.

Abstract

Functional reorganization of brain cortical areas occurs following stroke in humans, and many instances of this plasticity are associated with recovery of function. Rodent studies have shown that following a cortical stroke, neurons in uninjured areas of the brain are capable of sprouting new axons into areas previously innervated by injured cortex. The pattern and extent of structural plasticity depend on the species, experimental model, and lesion localization. In this study, we examined the pattern of axon sprouting in spinal cord after a localized lesion which selectively targeted the primary motor cortex in adult mice. We subjected mice to a stereotaxic-guided photothrombotic stroke of the left motor cortex, followed 2 weeks later by an injection of the neuronal tracer biotinylated dextran amine (BDA) into the uninjured right motor cortex. BDA-positive axons originating from the uninjured motor cortex were increased in the gray matter of the right cervical spinal cord in stroke mice, compared to sham control mice. These results show that axon sprouting can occur in the spinal cord of adult wild-type mice after a localized stroke in motor cortex.

Keywords

stroke; axon sprouting; spinal cord; photothrombosis.

Stroke is one of the leading causes of long-term disability in the United States [32]. Fortunately, many stroke patients experience some degree of recovery. One mechanism thought to underlie recovery is axon sprouting and the formation of new axon pathways. Imaging studies have shown reorganization of cortical areas following brain injury in humans, including stroke [reviewed in 9], and in many cases this plasticity is correlated with recovery [reviewed in 30]. Recovery after motor cortex injury is of particular interest because this region is commonly affected in human strokes, and often results in devastating functional deficits related to impaired control of the contralateral face, arm, and leg [24]. While it is possible that changes in activation patterns seen with MRI, PET, and transcranial magnetic stimulation after stroke could be due solely to changes in existing synapses, neuronal tracer studies in rodents indicate that new anatomical connections are formed after stroke.

There is considerable evidence from rat models that axon sprouting can occur in untreated animals after stroke. Stroke in sensorimotor cortex induced sprouting of axons from contralateral cortical neurons into the peri-infarct cortex and underlying denervated striatum

Address correspondence to: Mark P. Goldberg goldbergm@neuro.wustl.edu Telephone: 314-362-3258 Fax: 314-362-9462.

[6,25,39]. Liu and colleagues [21] showed that rat middle cerebral artery occlusion (MCAo) was followed by sprouting of axons from the uninfarcted hemisphere into denervated spinal cord, even in untreated control rats. The MCAo model injured both cortical and subcortical structures, and it is not known whether a lesion confined to cortex alone would be sufficient to trigger sprouting in spinal cord. These studies demonstrate unique patterns of distal axon sprouting after different types of ischemic lesions in rats.

While most experimental stroke studies have been performed in rats, mouse models provide opportunities for studying recovery mechanisms in transgenic animals. Mouse stroke models are more technically challenging and fewer studies of post-stroke axon sprouting are available. Riban and Chesselet [29] observed sprouting in mouse striatum after focal lesion in the ipsilateral sensorimotor cortex. Lee et al. [16] described sprouting in spinal cord of Nogo-A/B or Nogo receptor heterozygous mice after a photothrombosis lesion.

We set out to assess whether spontaneous spinal axon sprouting also occurs in wild-type mice, after a focal ischemic lesion anatomically targeted to primary motor cortex. The rodent MCAo model may induce considerable variability in infarct sizes, and does not consistently injure the primary motor area [unpublished observations and 3,22,31,36,38]. Therefore, we used a photothrombosis model, in which transcranial illumination by a stereotaxic fiber optic probe activates a systemically administered dye, rose bengal, triggering intravascular coagulation. Some of this work has been presented in abstract form [15].

For this study, 10 adult male C57Bl/6 mice (14 weeks old, Jackson Laboratory, Bar Harbor, ME) were used: five underwent stroke surgery, and five underwent sham surgery. One stroke mouse was excluded because the tracer injection did not label layers II/III through V, one stroke mouse was excluded because the lesion did not completely injure layer V, and one sham mouse died. In total, 7 mice were analyzed for sprouting in spinal cord (4 sham and 3 stroke mice). All procedures involving vertebrate animals were performed in accordance with the Institute of Laboratory Animal Research (ILAR) Guide for the Care and Use of Laboratory Animals, and procedures were approved by the Institutional Animal Studies Committee at Washington University School of Medicine.

The photothrombotic stroke model used was based on that of Watson et al. [40] and Schroeter et al. [34]. Mice were anesthetized with 1.75% isoflurane in room air and body temperature maintained at 37.0 ± 0.5 °C. The animal was positioned in a three-point fixation stereotaxic frame and a midline incision was made in the scalp. One end of a 1.0 m long fiber optic cable with 2 SMA-type ends and a 1.5 mm diameter (0.37 numerical aperture) core (BFH37-1500, Thorlabs Inc., Newton, NJ) was attached to a lamp housing (Fostec) with EKE-type halogen bulb (150W) and the other end was attached to the stereotaxic frame. A hot mirror (passes ~375-750 nm; Part 21002b; Chroma Technology Corp., Rockingham, VT) was placed within the path of light to reflect ultra-violet and infrared light and reduce the amount of heat delivered to the brain. After placing the fiber optic (with light off) on the skull directly above the left motor cortex (coordinates: anterior/posterior (a/p): +1.1 mm, medial/lateral (m/l): +1.5 mm; [20,27]), the mouse received an intraperitoneal injection of 200 μL of 20 mg/mL rose bengal dye (4,5,6,7-Tetrachloro-2′,4′,5′,7′-tetraiodofluorescein sodium salt; Sigma, St. Louis, MO) in phosphate buffered saline (PBS). After 1 min, the lamp was turned on and skull overlying the motor cortex was illuminated for 15 min. Sham mice were treated the same, except the lamp was not turned on.

The light power was adjusted prior to placement of the fiber using a LaserCheck light meter (Coherent Inc., Santa Clara, CA) calibrated to the wavelength corresponding to the maximum absorption peak of the rose bengal dye (562 nm) [4]. For these experiments, the lamp was set to provide 50 mW output light intensity, with a light fluence of 2.8 W/cm^2 and total exposed

energy density of 2.52 kJ/ cm^2. The effective photothrombotic dose is proportional to the fluence within the rose bengal dye absorption band, which can be approximated by normalizing the full fluence by the ratio (0.08) of the spectral width of the rose bengal absorption (30 nm) [14] to the spectral width of the illumination light (375 nm). Using this normalization the effective light levels are a fluence of 224 mW/cm^2 and a total dose of 202 J/cm^2.

Two weeks after photothrombosis, mice were anesthetized as described above and placed in the stereotaxic frame. A 1 mm burr hole was made in the skull above the right motor cortex (a/p: +1.1 mm, m/l: −1.5 mm, dorsal ventral (d/v): −1.6 [20,27]. A 5 μL Hamilton microsyringe with a 33 gauge needle with 45° tip (Hamilton Co., Reno, NV) was controlled by a nanoinjector pump (Stoelting Co., Wood Dale, IL) and used to inject 1.5 μL of 10% biotinylated dextran amine (10,000 MW BDA; Molecular Probes, Carlsbad, CA) in PBS at 0.15 μL/min. The needle was withdrawn 5 min post-infusion.

Mice were sacrificed 2 weeks post-injection of BDA (4 weeks after photothrombosis). Mice were anesthetized with ketamine and xylazine then transcardially perfused with PBS followed by 4% paraformaldehyde (Electron Microscopy Sciences, Hartfield, PA) in 0.1 M phosphate buffer. Brain and spinal column were fixed overnight in 4% paraformaldehyde. The next day, the spinal cords were dissected out of the vertebrae and brains and spinal cords were separately coded to blind the experimenters to the experimental group. Tissue was cryoprotected through graded concentrations of sucrose, embedded in OCT (Sakura Finetek U.S.A., Inc., Torrance, CA) and frozen. Tissue was sectioned coronally at 16 μm on a cryostat microtome. Every 12^{th} brain section was stained with cresyl violet Nissl stain to visualize infarcts. Briefly, frozen sections were rinsed in water, incubated for 10 min in 0.25% cresyl violet acetate solution (pH 3.6), rinsed in water, incubated in 95% ethanol, 100% ethanol, xylenes, then coverslipped with Permount (Fisher Scientific). Every 50^{th} cervical spinal cord section was incubated as follows to visualize the BDA: 3% hydrogen peroxide in 90% methanol to block endogenous peroxidases, Streptavidin-HRP (horseradish-peroxidase; diluted 1:500; Perkin Elmer) followed by 0.05% 3,3′-diaminobenzidine tetrahydrochloride, dihydrate (DAB), and 0.003% hydrogen peroxide.

Digital photographs of tissue were taken using a light microscope (Nikon TE300) and Spot Camera and software (Diagnostic Instruments, Inc., Sterling Heights, MI). Images of Nissl-stained brain sections (every 12^{th} section) were taken as montages with a 4X objective and infarct area in the left hemisphere was measured with Metamorph Imaging software.

Montage digital photographs of the cervical spinal cord (every 50^{th} section, 6 - 11 sections per mouse) were taken with a 10X objective. Experimenters were further blinded from whether images were from the same mouse. BDA^+ axon length (in μm) was quantified in the right and left gray matter and dorsal corticospinal tract (dCST) using Metamorph Imaging software. In addition, a thresholding function was used to highlight BDA^+ pixels and measure total BDA^+ surface area (in μm^2) in right and left cervical dCST. To account for possible variability in injection volume between animals, the amount of BDA label in each section was expressed as a ratio: right/left (ipsilateral to injection/contralateral). The ratios were averaged for each animal and then sham and stroke groups were compared using a Student's t-test. Errors are standard error of the mean.

At 35 days after photothrombotic stroke, ischemic lesions were visible in an anatomical area corresponding to forelimb motor cortex [20,27] (Fig. 1). Sham-treated brains did not show any signs of injury (Fig. 1). Nissl staining showed infarcts with a maximum width of 1.2 ± 0.2 mm (medial to lateral) (Fig. 1B) and an average length of 1.2 ± 0.2 mm (anterior to posterior; Fig. 1C). Therefore, the average infarct size was slightly smaller than the diameter of the 1.5 mm fiber optic. The lesion reached through at least layer V in the 3 stroke mice analyzed. The

photothrombosis lesions resulted in a cystic core surrounded by increased cellularity as identified by a nuclear stain (data not shown) or Nissl stain (Fig. 1B). Many of these cells were Iba-1-positive microglia (data not shown).

The neuronal tracer BDA typically labeled cells throughout all layers of the cortex and the BDA injections did not appear to spread to the underlying white matter. All mice analyzed had BDA-labeled cell bodies in layer V that were located at the same anterior-posterior level as the lesion.

Previous studies have shown post-stroke axon sprouting after cortical lesions in spinal cord of rats [21] and genetically-modified mice [16], so we asked whether spinal axon sprouting also occurs in wild-type mice. Four weeks after photothrombosis of left motor cortex and 2 weeks after injection of BDA into right motor cortex, BDA^+ axon length was measured in the right and left halves of cervical spinal cord gray matter. In shams, neurons labeled with BDA in the right motor cortex sent axons that projected mainly through the left dorsal corticospinal tract (dCST), with just a few axon fragments visible in right dCST (Fig. 2A and C). Axons in sham animals projected to the gray matter within the cervical spinal cord, mainly to the left half of the spinal cord (Fig. 2A and C). Very few BDA^+ axons were seen at thoracic levels of spinal cord (data not shown). The average BDA^+ axon length ratio of right to left gray matter in sham animals was 0.018 ± 0.004.

In stroke animals, the distribution of BDA^+ axons within the white matter was similar to that observed in sham animals (Fig. 2B and D). However, after stroke, BDA^+ axon length increased within the right spinal cord gray matter (Fig. 2B and D). The ratio of BDA^+ axon length (right/left) after stroke was statistically higher than this ratio in shams (0.046 ± 0.003 versus 0.018 ± 0.004; $p = 0.003$; Fig. 2E). The number of BDA+ fibers (ratio of right/left) was also somewhat increased after stroke, but this was not statistically significant (0.05 ± 0.01 versus 0.03 ± 0.02).

We considered sources of "new" BDA^+ axons seen within right (ipsilateral to injection) spinal cord gray matter. Previous studies suggest that axons likely cross the spinal midline near the level where they terminate in the gray matter [2,33,43], but to rule out long distance axon growth along the right dCST, we measured both BDA^+ axon length and BDA^+ pixels (as separate methods of measurement) within right and left cervical dCST and expressed each (separately) as a ratio of right to left. For both methods of analysis, there was no statistical difference between the ratios of shams (axon length ratio: 0.013 ± 0.007; BDA^+ pixels ratio: 0.008 ± 0.006) and stroke mice (axon length ratio: 0.012 ± 0.006, $p = 0.952$; BDA^+ pixels ratio: 0.006 ± 0.003, $p = 0.784$; axon length ratios shown in Fig. 2F). This observation suggests that additional axons found in the ipsilateral spinal cord after stroke were derived from axons branching at the spinal level.

To determine whether BDA^+ axons in left spinal cord gray matter cross the midline, we counted BDA^+ axons crossing a 1-pixel line at the midline. In total we observed only 5 "crossing" axons in 7 sham and stroke mice. While there was no significant difference between the groups in crossing axons per section (0.06 ± 0.06 for stroke versus 0.2 ± 0.1 for sham; $p = 0.454$), this comparison should be interpreted cautiously because we counted very few crossing events in either group.

We used a model of photothrombotic stroke to selectively injure the left motor cortex of the adult wild-type mouse while sparing the striatum, and show that this lesion induced uninjured right corticospinal axons to sprout into contralateral spinal cord gray matter.

The photothrombotic method reliably induced a lesion localized to motor cortex. Stereotaxic coordinates for the stroke and BDA injection were based on a brain atlas [27] and a previous study in mouse using intracortical microstimulation [20]. BDA^+ axons were seen projecting

through the dCST but not other spinal cord white matter tracts, and very few BDA^+ axons were seen at thoracic levels of the spinal cord. These observations indicate our studies targeted the corticospinal neurons corresponding to the forelimb motor representation. While photothrombosis does not perfectly mimic clinical stroke, it shares many characteristics with it and provides advantages over other stroke models. Arterial occlusion models, which depend on the distribution and overlap of vascular supply,can yield considerable variability in infarct size and do not consistently injure the primary motor area [unpublished observations and 3, 22,31,36,38]. In this study, the small size of the optical fiber (1.5 mm) produced a smaller lesion than observed with other stroke models. A smaller lesion can improve post-stroke survival, which is valuable for examining axon sprouting and functional recovery. The limited lesion is also representative of many human strokes, which typically affect approximately 4.5 to 14% of the hemisphere [5].

We found that the ratio of BDA axon length (right/left) in the gray matter was increased 4 weeks after stroke, demonstrating that new BDA^+ axons sprouted within the right spinal cord gray matter. The time point used in our study (2 weeks post-BDA injection and 4 weeks post-stroke) closely follows previous work in similar models. In other studies that show post-stroke axon sprouting, BDA was transported anterogradely to distal axons in rodent spinal cord within 1 to 2 weeks [8,16,29,43] after injection and sprouting was evident at 18, 32 (in mouse striatum) [29], and 28 days (in mutant mouse spinal cord) [16] after stroke.

Axon sprouting after injury is dependent on animal age, species, and injury model. Previous studies have demonstrated that the uninjured hemisphere is capable of sending projections to the ipsilateral spinal cord following a unilateral cortical lesion in neonatal rats [2,7,10-12, 17-19,23,28,33,42] or adult rodents with axon growth-inhibiting molecules knocked-out or neutralized with antibodies [16,26,35,41,43]. However, in several unilateral brain injury models using wild-type adult rodents, the opposite hemisphere was not involved in recovery and ipsilateral projections in the spinal cord were not observed [1,2,10,11,13,18,42]. These experiments used non-ischemic methods of brain injury (hemispherectomy, aspiration, or electrolytic lesions) which may have influenced the occurrence of axon sprouting (for example, it occurs after ischemic but not aspiration lesions [6,25,37,39]). In agreement with studies of rat MCAo [21], our results with mouse photothrombotic stroke support the presence of post-ischemic sprouting of uninjured corticospinal axons in the spinal cord of adult animals.

In conclusion, we show that a photothrombotic stroke in left motor cortex of wild-type mice induced sprouting from uninjured right corticospinal axons into the right spinal cord gray matter. The ability to place ischemic lesions within an anatomically delimited brain region aids in defining roles of specific neuron pathways in post-stroke recovery. In the current study, we establish that direct striatal injury is not required for corticospinal axon sprouting after stroke and that axon sprouting occurs in regions distant from the cortical lesion in mice. This model of spontaneous axon sprouting in mouse spinal cord provides opportunities to examine unique signaling pathways which trigger sprouting by uninjured axons.

Acknowledgments

We thank Benjamin Zeff, Dr. Tanya Tenkova, and Hank H. Sun for technical assistance. We thank Ernie Gonzales, Jin-Moo Lee, and the Animal Models Core at the Hope Center for Neurological Disorders for providing and maintaining facilities necessary for this study.

Funding was provided by the American Heart Association – 0615509Z (CMLD) and grants from the National Institutes of Health – P01 NS032636 (MPG), R01 NS36265 (MPG), P30 NS057105 (MPG), K25 NS4339 (JPC) and R21 EB007924 (JPC).

References

1. Barth TM, Jones TA, Schallert T. Functional subdivisions of the rat somatic sensorimotor cortex. Behav. Brain Res 1990;39:73–95. [PubMed: 2390194]
2. Barth TM, Stanfield BB. The recovery of forelimb-placing behavior in rats with neonatal unilateral cortical damage involves the remaining hemisphere. J Neurosci 1990;10:3449–3459. [PubMed: 2213147]
3. Bederson JB, Pitts LH, Tsuji M, Nishimura MC, Davis RL, Bartkowski H. Rat middle cerebral artery occlusion: evaluation of the model and development of a neurologic examination. Stroke 1986;17:472–476. [PubMed: 3715945]
4. Boquillon M, Boquillon JP, Bralet J. Photochemically induced, graded cerebral infarction in the mouse by laser irradiation evolution of brain edema. J Pharmacol. Toxicol. Methods 1992;27:1–6. [PubMed: 1581608]
5. Carmichael ST. Rodent models of focal stroke: size, mechanism, and purpose. NeuroRx 2005;2:396–409. [PubMed: 16389304]
6. Carmichael ST, Chesselet MF. Synchronous neuronal activity is a signal for axonal sprouting after cortical lesions in the adult. J. Neurosci 2002;22:6062–6070. [PubMed: 12122067]
7. Castro AJ. Ipsilateral corticospinal projections after large lesions of the cerebral hemisphere in neonatal rats. Exp. Neurol 1975;46:1–8. [PubMed: 1109332]
8. Chen P, Goldberg DE, Kolb B, Lanser M, Benowitz LI. Inosine induces axonal rewiring and improves behavioral outcome after stroke. Proc. Natl. Acad. Sci. U. S. A 2002;99:9031–9036. [PubMed: 12084941]
9. Hallett M. Plasticity of the human motor cortex and recovery from stroke. Brain Research Reviews 2001;36:169–174. [PubMed: 11690613]
10. Hicks SP, D'Amato CJ. Motor-sensory and visual behavior after hemispherectomy in newborn and mature rats. Exp. Neurol 1970;29:416–438. [PubMed: 5492916]
11. Hicks SP, D'Amato CJ. Motor-sensory cortex-corticospinal system and developing locomotion and placing in rats. Am. J Anat 1975;143:1–42. [PubMed: 48336]
12. Huttenlocher PR, Raichelson RM. Effects of neonatal hemispherectomy on location and number of corticospinal neurons in the rat. Brain Res. Dev. Brain Res 1989;47:59–69.
13. Kartje-Tillotson G, Neafsey EJ, Castro AJ. Electrophysiological analysis of motor cortical plasticity after cortical lesions in newborn rats. Brain Res 1985;332:103–111. [PubMed: 3995256]
14. Khajehpour M, Troxler T, Vanderkooi JM. Probing the active site of trypsin with rose bengal: insights into the photodynamic inactivation of the enzyme. Photochem. Photobiol 2004;80:359–365. [PubMed: 15244504]
15. LaPash CM, Ayers KL, Finley AM, Goldberg MP. Axon sprouting in mouse spinal cord after cortical stroke 2007. Neuroscience Meeting Planner 55 2007;17
16. Lee JK, Kim JE, Sivula M, Strittmatter SM. Nogo receptor antagonism promotes stroke recovery by enhancing axonal plasticity. J. Neurosci 2004;24:6209–6217. [PubMed: 15240813]
17. Leong SK. A qualitative electron microscopic investigation of the anomalous corticofugal projections following neonatal lesions in the albino rats. Brain Res 1976;107:1–8. [PubMed: 1268714]
18. Leong SK. An experimental study of the corticofugal system following cerebral lesions in the albino rats. Exp. Brain Res 1976;26:235–247. [PubMed: 991955]
19. Leong SK, Lund RD. Anomalous bilateral corticofugal pathways in albino rats after neonatal lesions. Brain Res 1973;62:218–221. [PubMed: 4765111]
20. Li CX, Waters RS. Organization of the mouse motor cortex studied by retrograde tracing and intracortical microstimulation (ICMS) mapping. Can. J Neurol. Sci 1991;18:28–38. [PubMed: 2036613]
21. Liu Z, Li Y, Qu R, Shen L, Gao Q, Zhang X, Lu M, Savant-Bhonsale S, Borneman J, Chopp M. Axonal sprouting into the denervated spinal cord and synaptic and postsynaptic protein expression in the spinal cord after transplantation of bone marrow stromal cell in stroke rats. Brain Res 2007;1149:172–180. [PubMed: 17362881]
22. Longa EZ, Weinstein PR, Carlson S, Cummins R. Reversible middle cerebral artery occlusion without craniectomy in rats. Stroke 1989;20:84–91. [PubMed: 2643202]

23. McClung JR, Castro AJ. An ultrastructural study of ipsilateral corticospinal terminations in the rat. Brain Res 1975;89:327–330. [PubMed: 1148852]
24. Mohr, JP.; Choi, DW.; Grotta, JC.; Weir, B.; Wolf, PA. Stroke Pathophysiology, Diagnosis, and Management. Churchill Livingstone; Philadelphia: 2004.
25. Napieralski JA, Butler AK, Chesselet MF. Anatomical and functional evidence for lesion-specific sprouting of corticostriatal input in the adult rat. Journal of Comparative Neurology 1996;373:484–497. [PubMed: 8889940]
26. Papadopoulos CM, Tsai SY, Alsbiei T, O'Brien TE, Schwab ME, Kartje GL. Functional recovery and neuroanatomical plasticity following middle cerebral artery occlusion and IN-1 antibody treatment in the adult rat. Ann. Neurol 2002;51:433–441. [PubMed: 11921049]
27. Paxinos, G.; Franklin, BJ. The Mouse Brain in Stereotaxic Coordinates. Vol. 2nd edition. Academic Press; San Diego: 2001.
28. Reinoso BS, Castro AJ. A study of corticospinal remodelling using retrograde fluorescent tracers in rats. Exp. Brain Res 1989;74:387–394. [PubMed: 2924858]
29. Riban V, Chesselet MF. Region-specific sprouting of crossed corticofugal fibers after unilateral cortical lesions in adult mice. Exp. Neurol 2006;197:451–457. [PubMed: 16321385]
30. Rijntjes M. Mechanisms of recovery in stroke patients with hemiparesis or aphasia: new insights, old questions and the meaning of therapies. Curr. Opin. Neurol 2006;19:76–83. [PubMed: 16415681]
31. Robinson MJ, Macrae IM, Todd M, Reid JL, McCulloch J. Reduction of local cerebral blood flow to pathological levels by endothelin-1 applied to the middle cerebral artery in the rat. Neurosci. Lett 1990;118:269–272. [PubMed: 2274283]
32. Rosamond W, Flegal K, Furie K, Go A, Greenlund K, Haase N, Hailpern SM, Ho M, Howard V, Kissela B, Kittner S, Lloyd-Jones D, McDermott M, Meigs J, Moy C, Nichol G, O'Donnell C, Roger V, Sorlie P, Steinberger J, Thom T, Wilson M, Hong Y. Heart disease and stroke statistics--2008 update: a report from the American Heart Association Statistics Committee and Stroke Statistics Subcommittee. Circulation 2008;117:e25–146. [PubMed: 18086926]
33. Rouiller EM, Liang FY, Moret V, Wiesendanger M. Trajectory of redirected corticospinal axons after unilateral lesion of the sensorimotor cortex in neonatal rat; a phaseolus vulgaris-leucoagglutinin (PHA-L) tracing study. Exp. Neurol 1991;114:53–65. [PubMed: 1915735]
34. Schroeter M, Jander S, Stoll G. Non-invasive induction of focal cerebral ischemia in mice by photothrombosis of cortical microvessels: characterization of inflammatory responses. Journal of Neuroscience Methods 2002;117:43–49. [PubMed: 12084563]
35. Seymour AB, Andrews EM, Tsai SY, Markus TM, Bollnow MR, Brenneman MM, O'Brien TE, Castro AJ, Schwab ME, Kartje GL. Delayed treatment with monoclonal antibody IN-1 1 week after stroke results in recovery of function and corticorubral plasticity in adult rats. J Cereb. Blood Flow Metab 2005;25:1366–1375. [PubMed: 15889044]
36. Shigeno T, Teasdale GM, McCulloch J, Graham DI. Recirculation model following MCA occlusion in rats. Cerebral blood flow, cerebrovascular permeability, and brain edema. J Neurosurg 1985;63:272–277. [PubMed: 4020448]
37. Szele FG, Alexander C, Chesselet MF. Expression of Molecules Associated with Neuronal Plasticity in the Striatum After Aspiration and Thermocoagulatory Lesions of the Cerebral-Cortex in Adult-Rats. J. Neurosci 1995;15:4429–4448. [PubMed: 7790918]
38. Tamura A, Graham DI, McCulloch J, Teasdale GM. Focal cerebral ischaemia in the rat: 1. Description of technique and early neuropathological consequences following middle cerebral artery occlusion. J Cereb. Blood Flow Metab 1981;1:53–60. [PubMed: 7328138]
39. Uryu K, MacKenzie L, Chesselet MF. Ultrastructural evidence for differential axonal sprouting in the striatum after thermocoagulatory and aspiration lesions of the cerebral cortex in adult rats. Neuroscience 2001;105:307–316. [PubMed: 11672598]
40. Watson BD, Dietrich WD, Busto R, Wachtel MS, Ginsberg MD. Induction of reproducible brain infarction by photochemically initiated thrombosis. Ann. Neurol 1985;17:497–504. [PubMed: 4004172]
41. Wenk CA, Thallmair M, Kartje GL, Schwab ME. Increased corticofugal plasticity after unilateral cortical lesions combined with neutralization of the IN-1 antigen in adult rats. J Comp Neurol 1999;410:143–157. [PubMed: 10397401]

42. Whishaw IQ, Kolb B. Sparing of skilled forelimb reaching and corticospinal projections after neonatal motor cortex removal or hemidecortication in the rat: support for the Kennard doctrine. Brain Res 1988;451:97–114. [PubMed: 3251605]

43. Wiessner C, Bareyre FM, Allegrini PR, Mir AK, Frentzel S, Zurini M, Schnell L, Oertle T, Schwab ME. Anti-Nogo-A antibody infusion 24 hours after experimental stroke improved behavioral outcome and corticospinal plasticity in normotensive and spontaneously hypertensive rats. J Cereb. Blood Flow Metab 2003;23:154–165. [PubMed: 12571447]

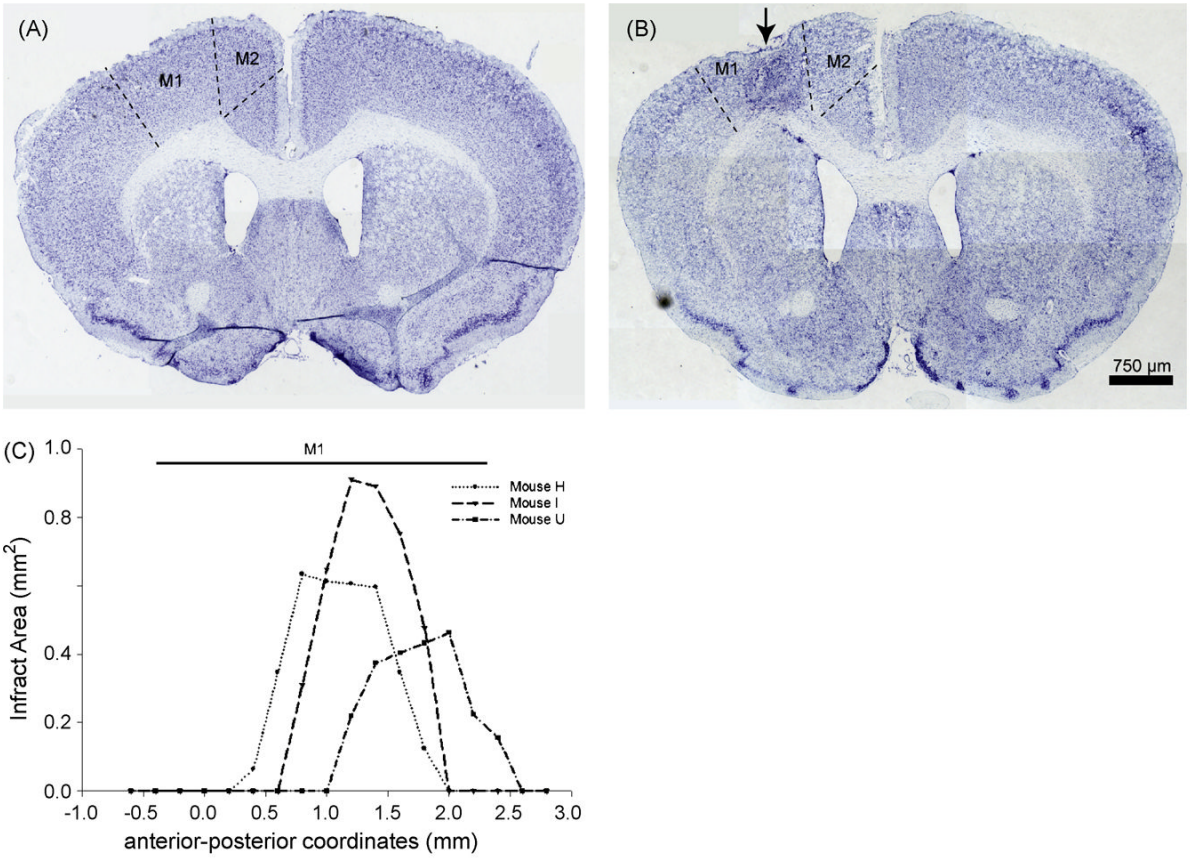

Figure 1. Photothrombotic stroke targets motor cortex

A. Sham operation does not result in any damage to cortex, as seen with a Nissl stain. B. Using stereotaxic placement of a fiber optic, an infarct (arrow) can be localized within the primary motor cortex (M1). C. Infarct area at points along the anterior-posterior (a-p) axis. The average a-p extent of the lesions was 1.2 ± 0.2 mm. The line above the graph shows the extent (in the a-p axis) of M1 where it would be targeted by a 0.5 mm wide (medial to lateral) lesion centered at 1.5 mm lateral to the midline. M1, primary motor cortex; M2, secondary motor cortex.

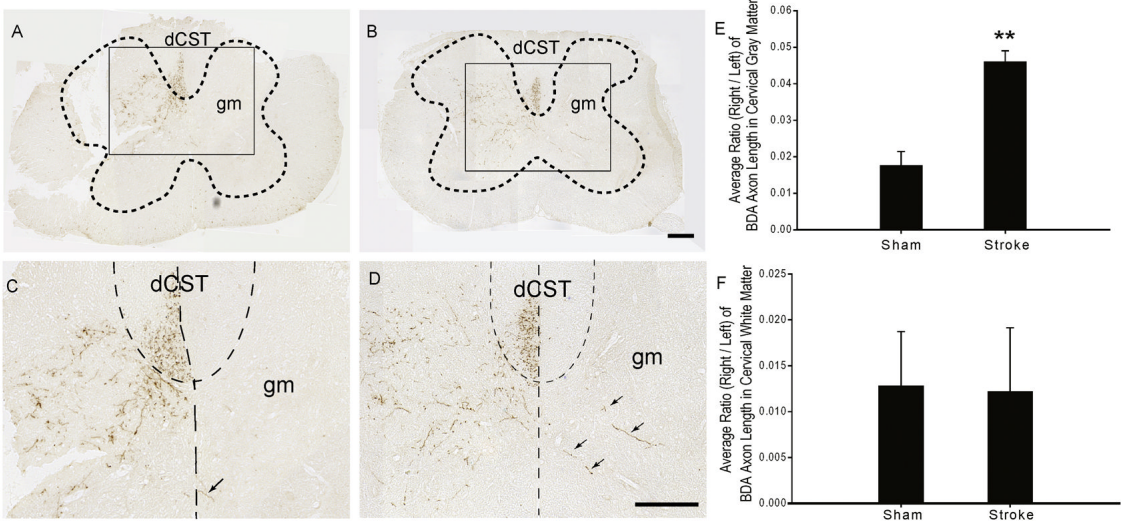

Figure 2. BDA-labeled axons from right motor cortex are increased in ipsilateral cervical spinal cord gray matter 4 weeks after left motor cortex stroke

A, B. Low-power images of spinal cord cervical sections 4 weeks after sham operation (A) or photothrombotic stroke (B) over left motor cortex and 2 weeks after injection of BDA in right motor cortex. BDA+ axon length was measured in left and right cervical spinal cord gray matter (gm, outlined by the dotted lines) or dorsal corticospinal tract (dCST). The rectangular outlined areas in A and B are shown at higher magnification in C and D, respectively. C, D. Higher-power images of spinal cord 4 weeks after sham (C) or stroke (D). Vertical dotted lines delineate the midline and curved dotted lines separate the white matter dCST from the gm. There is an increase in BDA+ axon length in the right gm after stroke (D) compared to sham (C) (arrows show examples of BDA+ axons). E. The average ratio of BDA+ axon length (right/left) in gm was statistically higher than the ratio of sham mice (0.046 ± 0.003 vs. 0.018 ± 0.004; $p = 0.003$). F. There was no significant difference in the average ratios of BDA+ axon length in dCST (right/left) between sham (0.013 ± 0.007) and stroke (0.012 ± 0.006) mice ($p = 0.952$). Scalebars in B and D are 200 μm.